Bulletin of Volcanology (2023) 85:35
https://doi.org/10.1007/s00445-023-01642-3

RESEARCH ARTICLE

Lessons learned from the 1980–1986 eruption of the Mount St. Helens composite lava dome

Jonathan Fink[1] · **Steven Anderson**[2]

Received: 29 November 2022 / Accepted: 28 March 2023 / Published online: 8 May 2023

Abstract
After its cataclysmic explosive eruptive activity on May 18, 1980, most of the output of Mount St. Helens (MSH) for the next six and a half years was quietly extruding lava, which built up one of the best documented and most instructive lava domes of the twentieth century. The unprecedented amount of data collected about the growth of the dome led to a profusion of new models and concepts. In this paper, we first describe some of the early mechanical models and then focus on three specific aspects of the emplacement of the MSH lava dome that were measurable in particularly great detail: the partitioning between exogenous and endogenous styles of growth; the distribution of vesicular textures and their relationship to volatile contents and eruptive conditions; and the presence of characteristic structural features like fractures, folds, and spines. Taken together, these three overlapping physical manifestations of magmatic behavior, evidence of which may be preserved in the geologic record or observed with remote sensing, can provide insights about whether a quietly extruding dome is likely to exhibit dangerous endogenic pyroclastic behavior.

Keywords Eruption · Domes · Mount St. Helens

Introduction

For the volcanological community of the USA, and to a lesser extent for the rest of the world, the 1980–1986 eruption of Mount St. Helens (WA) was a signature event. Before 1980, many volcano scientists from US universities and the US Geological Survey (USGS) received most of their professional training observing active mafic volcanism in Hawaii, or inferring prehistoric processes from dormant or extinct volcanoes in the western USA. Although many of these scientists were familiar with a range of explosive phenomena observed at volcanoes in Central America, Japan, Indonesia, and elsewhere, there had not been any violent eruptive events to witness in the conterminous USA since Mount Lassen ~ 60 years earlier. Thus, May 18th's sector collapse, landslide, Plinian column, surge, pyroclastic flows, and lahars, along with subsequent summit explosions that summer, received most of the scientific and public attention.

However, for most of the next six and a half years, the dominant volcanic process at MSH, and the easiest to observe, was the emergence of a series of lava dome lobes within the May 18 crater, culminating in a final extrusion that started in October 1980 and grew episodically until October 1986. Although several eruptions in Alaska over the preceding few decades had produced monitored lava domes (Siebert et al. 1995; Coombs et al. 2006; Bull et al. 2013; Bull and Buurman 2013), there had never been an active dome in the USA that could be as readily observed and instrumented by geoscientists as that of Mount St. Helens.

Globally, most previous dome studies focused on their association with violent collapse events that produced pyroclastic flows, as occurred at Mont Pelée on the island of Martinique in 1902, killing over 29,000 people (Boudon and Balcone-Boissard 2021). The Santiaguito dome complex on the side of Santa Maria Volcano in Guatemala, active since 1922, has produced several pyroclastic flows, in some cases

Editorial responsibility: U. Kueppers

This paper constitutes part of a topical collection: Over forty years since the May 1980 Mount Saint Helens eruption: Lessons, progress and perspectives

✉ Jonathan Fink
jon.fink@pdx.edu

[1] Department of Geology, Portland State University, Portland, OR, USA

[2] Department of Earth and Atmospheric Sciences, University of Northern Colorado, Greeley, CO, USA

from the fronts of lobes up to 2 km from the active vent (Rose et al. 1976; Rhodes et al. 2018). Deadly explosive collapse events take place on a decadal timescale from the summit dome of Indonesia's persistently active andesitic Merapi Volcano (Widiyantoro et al. 2018). Later well-documented eruptions at Mount Unzen in Japan (Nakada et al. 1999) and on the Soufrière Hills Volcano on Montserrat in the 1990s (Sparks and Young 2002) brought additional attention to these phenomena. These works form the foundation for our current understanding of dome growth, which now extends to submarine and planetary environments.

Although the 1980–1986 MSH dome did not generate any major explosive episodes, there were several smaller explosions (i.e., March 1982) that produced lahars that threatened downslope areas and contributed to ongoing anxiety about such risks throughout its growth. Partly because of this concern, the 1980–1986 MSH extrusion yielded data sets that formed the basis for dozens of later studies, including an extensive collection that focused on the 2004–2008 Mount St. Helens' dome growth (Sherrod et al. 2008). Much of the 1980–1986 work was led by USGS scientists, but we and other academic geologists were also able to contribute because of the relatively easy access to and extensive instrumentation of the MSH crater.

Monitoring the MSH dome

Dome emplacement can be characterized by several variables: chemical composition, volatile content, crystallinity, vesicularity, vent and conduit geometry, effusion rate and continuity, and surface structures. Each of these can change during an eruption, leading to an extremely diverse catalog of possible dome histories and appearances. The simplest domes have uniform chemistries and volatile contents, steady effusion rates during a single period of emplacement, conduits with circular cross-sections that extrude lava onto flat surfaces, homogeneous vesicular and crystalline textures, and a limited range of symmetrically arrayed surface structures. Most domes, including those at Mount St. Helens, undergo a considerably more involved evolution.

The MSH sequence began with relatively small and simple domes that became progressively more complex. Domes appeared in the crater after explosive episodes in June, August, and October 1980; the last of these formed the foundation for the composite dome that grew over the next 6 years through a combination of extrusion of lobes and endogenous inflation (Swanson et al. 1987). The domes' major-element composition was dacite with silica content of 62 to 65 weight percent, which decreased through 1981 and then steadily increased from 1982 to 1986 (Cashman and Taggart 1983). Plagioclase microlite populations remained nearly constant throughout the 6-year history of the dome (Cashman 1992). Amphibole crystals with reaction rims indicating relatively slow growth were interpreted to have come from lava that resided along the walls of the conduit before being carried into the dome, while crystals without rims were thought to be from lava that rose directly from depth into the dome (Rutherford and Hill 1993).

As will be described in more detail later, the lava surface displayed two distinct vesicular textures — smooth and scoriaceous — the relative proportions of which tended to vary systematically throughout the 6 years of activity, becoming progressively smoother (less vesicular) (Swanson et al. 1987; Anderson and Fink 1989; 1990). In addition, several other common silicic lava flow surface features, including spines and crease structures (Anderson and Fink 1992), were formed on the surfaces of some of these dome lobes and provided clues about emplacement processes.

Rather than emerging from a linear, dike-like fissure system, as has been the case with the currently active Santiaguito dome complex (Harris et al. 2003), the 2011–2012 Cordon Caulle flow in Chile (Farquharson et al. 2015), or several Holocene chains of rhyolitic obsidian flows in California and Oregon (Fink and Pollard 1983), the entire series of MSH domes and lobes appeared to come out of a cylindrical, pipe-like vent similar to that observed at Colima (Luhr and Carmichael 1980) and Guagua Pichincha (Colombier et al. 2022), first onto the relatively flat floor of the recently created crater, and later onto the top of the increasingly complex extrusion. Geophysical measurements along with observations of the growing dome implied a conduit ranging from 20- to 30-m wide at the surface of the dome (Swanson and Holcomb 1990).

The crater and dome were well-monitored by state-of-the-art instrumentation. Helicopter and fixed-wing aircraft regularly circled the vent area, collecting detailed photogrammetric data sets from which high-resolution topographic maps could later be constructed. Most importantly, many government and academic volcano scientists carefully chronicled the growth of the dome, through sampling, geophysical and geochemical instrumentation, and regular visits to the crater.

Several monitoring tools that help document dome emplacement today were *not* available in the early 1980s. There were no drones surveying the crater, and no readily available artificial intelligence algorithms available to handle datasets with millions of points (Burzynski et al. 2018). GPS networks were not yet operational. The Internet and email would not become widely used by volcanologists for another decade, there were no commercial cellular networks, and satellite transmission of data from the crater was generally absent (Koenig and Fink 2002). Standard surveying methods of the 1980s could yield dozens of sub-cm-scale topographic points per day. In contrast, terrestrial and airborne LiDAR datasets routinely used today are capable of capturing millions of such points in minutes (Lewinter et al. 2021). Most

types of geophysical and geochemical instruments were one or more orders of magnitude less sensitive than today. Yet despite these limitations, the volcanological community was able to gain significant and novel insights from emplacement of the MSH dome that informed major campaigns at several later dome eruptions (Calder et al. 2015).

Modeling the MSH dome

Volcanic modelers have been drawn to study simple lava domes because they tend to be better preserved than the unconsolidated pyroclastic products that pre- or post-date them, and their interpretation is more straightforward than deciphering larger, more complex extrusions. Many dome features offer clues that help scientists infer emplacement conditions for eruptions that were not observable, either because they occurred prehistorically, or because they took place in inaccessible areas, including submarine (Romagnoli et al. 2013; Ikegami et al. 2018) or extra-terrestrial settings (Pappalardo and Greeley 1995; Stofan et al. 2000; Wilson and Head 2003; Rampey et al. 2007; Quick et al. 2022). Lava domes have been used to derive relationships among magma rheology, dynamics, and morphology, to better understand eruption mechanisms and hazards. These analytical models have commonly been tested through comparison with complementary laboratory simulations using analog materials.

Mechanically, lava domes can be thought of as having a solidified outer crust that transitions to a more ductile interior, with the whole assemblage fully or partially enclosed within a three-dimensional envelope of loose talus blocks (Iverson 1990). These tripartite near-surface packages represent the upper part of a larger system that also includes the conduit and one or more magma reservoirs at depth.

The overall emplacement of a dome can be considered to have five stages. (1) Magma enters a feeding chamber from a deeper source. (2) This magma cools, crystallizes, vesiculates, stopes wall rocks, and solidifies, generating an eruptible, buoyant, volatile-enhanced batch. (3) This lighter magma either breaks its way to the surface (at the onset of an eruption) or rises up the conduit, forcing earlier and already more crystallized magma units up ahead of it. If enough gas and heat are lost — upward through the vent or laterally into fractured country rock — overpressure buildup is insufficient to allow fragmentation. (4) Before emerging, the rising magma batch may deform the crater floor (Chadwick and Swanson 1989), then intruding into or breaking its way to the surface of the earlier-erupted dome. (5) This fresh lava spreads, cools, partially solidifies, fractures, brecciates, folds, slumps, vesiculates, or explodes (Fink et al. 1990; Anderson et al. 1995). Combinations of direct observations and geophysical, geodetic, and geochemical monitoring attempt to track this complex set of processes (i.e., Swanson and Holcomb 1990). Dome growth is the most readily observable and modellable portion of this vertically arrayed system.

Different analytical studies have made various assumptions about the behavior of the three surficial components of domes. For example, Huppert et al. (1982) modeled the growth of the 1979 Soufrière of St. Vincent basaltic andesite dome as a radially symmetric, Newtonian viscous fluid spreading across a flat surface, and derived relationships for height and radius versus time. They considered two simple emplacement cases — either a fixed volume of lava spreading under its own weight, or a growing amount of lava with an effusion rate that steadily decreased. They concluded that the eruption stopped when the hydrostatic head associated with the height of the dome balanced the magmatic pressure driving the molten rock upward.

In 1990, five papers (Swanson and Holcomb 1990; Blake 1990; Anderson and Fink 1990; Iverson 1990; Denlinger 1990) about emplacement of the Mount St. Helens dome were published in Volume 2 of the International Association of Volcanology and Chemistry of the Earth's Interior (IAVCEI)'s *Proceedings in Volcanology* series, "Lava flows and domes" (Fink 1990). All drew on quantitative data carefully gathered and interpreted by Swanson and Holcomb (1990), who detailed the dome's episodic nature with measurements of how dome height, radius, volume, and shape changed with time. Among their many important conclusions was that the volumetric growth rate was approximately linear during three distinct periods of progressively decreasing flux (Fig. 1). In each of these phases, the volume of lava erupted was proportional to the repose interval since the previous episode. They also suggested that dome shape

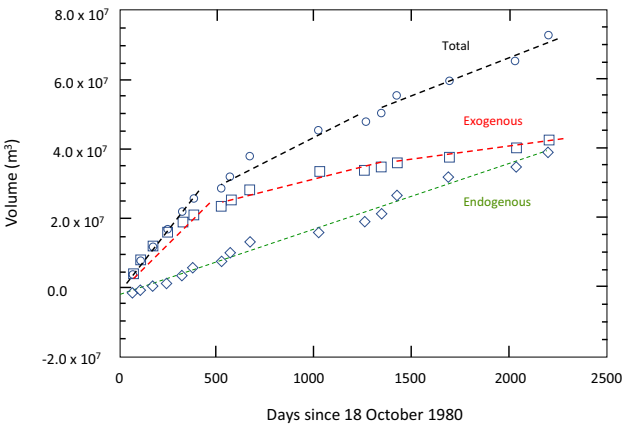

Fig. 1 Cumulative volume ($m.^3$) versus time of emplacement (in days since October 18, 1980) of the Mount St. Helens dome. Circles — total dome volume; squares — exogenous lobe volumes; diamonds — volume of endogenous inflation. Error bars on the volumes have been left off for clarity but are available in the references. Trend lines for total and exogenous volumes show three eruptive phases with decreasing eruption rates. Plot based on Fink et al. (1990)

(the ratio of height to radius) was controlled by the combined influence of the viscosity and strength of the core, outer crust, and surrounding talus apron. Finally, their data set showed that repose intervals steadily increased as the dome grew taller, suggesting that the increased lithostatic load required a greater amount of volatile-enriched magma to be generated before a new eruptive episode could begin (Anderson and Fink 1989).

Blake (1990) was one of the first to use a mechanical model to interpret the growth of the MSH dome. His study began by grouping an assortment of recent domes from around the world into four morphological classes, assuming they were composed of lava with a temperature-dependent, viscoplastic (Bingham) rheology, which deforms viscously when the applied stress exceeds a yield strength but behaves rigidly when stresses drop below this threshold. Blake distinguished between steep-sided Peléan domes, whose growth is controlled by the internal friction of the enclosing talus pile, and low lava domes, whose spreading is limited by the yield strength of the internal lava. He concluded that the likelihood of a dome experiencing explosive decompression depends on the same yield strength that controls its morphology. Peléan domes thus tend to generate pyroclastic flows, in contrast with low lava domes that are unable to support the higher stresses needed to allow a build-up of internal pressure. Although the MSH dome was quite steep when it stopped erupting in 1986, its individual lobes were relatively thin, leading Blake to classify them as being in the "low" grouping, less likely to experience explosive collapse.

In Iverson's (1990) view, the spreading of a dome depends primarily on the mechanical strength of its solid carapace. According to his model, domes expand volumetrically in a self-similar manner, retaining a ratio of height to diameter that is proportional to the tensile strength and thickness of the crustal layer, and to the internal pressure and density of the molten interior, independent of its rheology. He explained the transition from endogenous inflation to exogenous extrusion of lobes as depending on the pressurization of the interior lava. For lava to break through to the surface and form a new lobe, its pressure had to exceed the tensile strength of the crustal layer, which was in turn proportional to its thickness. This differed from Blake's (1990) model because Blake assumed that deformation can only occur when the internal pressure is greater than the yield strength of the lava rather than the tensile strength of the carapace.

Denlinger (1990) extended Iverson's (1990) model by focusing on how the fracture behavior of the crustal layer controlled when interior lava was able to break its way to the dome surface during an eruptive episode. He used fracture mechanics theory and various geophysical measurements of the May 1982 eruptive episode to calculate when the slowly stretching carapace of the inflating dome would suddenly rupture, allowing fresh lava to emerge to form a new lobe. He looked at the relative speed of growth of small cracks compared to larger ones and reviewed literature that describes how these processes can lead to catastrophic failure. His modeling showed that fracturing is far more likely to occur on the top of the dome than on its flanks, a finding consistent with observations at MSH.

This sequence of mechanical models each tried to incorporate an additional type of observation to understand how the appearance and behavior of the active MSH dome could provide clues about processes occurring in the underlying magma system, including within the interior of the dome itself. However, these formulations assumed steady-state processes that changed linearly with time. A series of later analyses considered the dynamics of dome growth, including feedback loops involving crystallization, viscosity increases, and the rate of magma rise through the conduit (Melnik and Sparks 1999, 2005; Barmin et al. 2002). Other recent studies of rhyolitic lavas and attendant explosive degassing (Castro et al. 2013; Schipper et al. 2013; Tuffen et al. 2013) identified nonlinear processes that could provide insights into hidden variables like the size of the magma body at depth and the nature of degassing processes occurring beneath the surface. All of these works built on earlier debates about whether domes emerge as permeable foams that compress to form glass as they flow (e.g., Taylor et al. 1983; Eichelberger et al. 1986) or as coherent lava that inflates through vesiculation (e.g., Fink et al. 1992).

In the rest of this paper, we review and synthesize three earlier studies of dome emplacement, which added several new constraints to the static mechanical models described above, including image processing that quantified the partitioning between endogenous and exogenous growth (Swanson and Holcomb, 1990; Fink et al. 1990); hydrogen isotope studies that revealed the relationship between lava texture and volatile content (Anderson and Fink 1989, 1990; Anderson et al. 1995; Hoblitt and Harmon 1993; Underwood et al. 2013); and analog experiments that explained how dome surface structures depend on the ratio of magma eruption rate to cooling rate (Griffiths and Fink 1997; Fink and Griffiths 1998; Lyman et al. 2004; Anderson et al. 2005). In addition to explaining aspects of the MSH dome eruption, these studies also provide insight into the subsequent growth of lava domes documented at Santiaguito in Guatemala (Anderson et al. 1995), Redoubt in Alaska (USA) (Bull et al. 2013), Shiveluch in Kamchatka (Russia) (Ramsey et al. 2012), Unzen in Japan (Nakada et al. 1995), and Soufrière Hills on Montserrat (Watts et al. 2002). Our interpretation is largely compatible with the recent comprehensive model presented by Wadsworth et al. (2022), based on observations of the Cordón Caulle (Tuffen et al. 2013) and Chaiten (Pallister et al. 2013) eruptions, which describes silicic flows as the products of hybrid explosive/effusive events.

Changes in eruptive style

The modeling studies described above looked at the conditions associated with two styles of dome growth, extrusion of exogenous lobes and intrusion via endogenous inflation. In one of the first volcanological studies to use volume differencing of digital topography to estimate erupted volumes, Fink et al. (1990) used topographic maps generated from sequential high-resolution imagery of the MSH dome collected by Robin Holcomb of the USGS to estimate how much of each eruptive phase was endogenous and how much was exogenous. The calculations required what was then state-of-the-art image processing to subtract the volume increases within an observed extrusive lobe from the measured overall growth; the difference was assumed equal to the amount of endogenous inflation. To our knowledge, this remains one of only two domes for which the partitioning between these two modes of growth has been accurately calculated; Kaneko et al. (2002) did a similar analysis of exogenous/endogenous partitioning at Mt. Unzen.

Figure 1 shows volume (in cubic meters) versus time (in days since October 18, 1980) for the overall dome (circles), the exogenous lobes (squares), and endogenous inflation (diamonds), along with approximate trend lines. Direct observations showed that the eruptive style shifted from early episodes dominated by formation of exogenous lobes to later periods in which increasing amounts of magma remained in the interior of the growing dome. This general trend would be expected, given that a small dome has less internal space than a large one to accommodate new magma before rupturing. However, our study revealed that the two modes exhibited quantitatively different fundamental patterns.

The cumulative volume increase of the exogenous lobes paralleled that of the overall dome, with three phases of constant eruption rate, in which each successive phase had a lower rate than its predecessor. This decrease was likely controlled by factors in the magmatic plumbing system identified by Swanson and Holcomb (1990). According to their interpretation, the first transition, at the end of 1981, accompanied a shift in the trend of lava composition from progressively more mafic to more silicic, suggesting that a fresh batch of slightly more silicic magma had been injected at depth. This next phase began with a significant explosion on March 19, 1982, reflecting the likely presence of more volatiles in this second batch of magma. This part of the eruption included the only period of extensive continuous endogenous inflation, which lasted for more than a year. The third phase of mostly endogenous dome growth produced progressively smaller lobes of exogenous lava with predominantly smooth rather than scoriaceous surface textures (see next section), and steadily lengthening repose periods. These observations imply that the final stage of dome emplacement involved magma that was relatively volatile-depleted.

Swanson and Holcomb (1990) suggested that during each of the three phases, the overall effusion rate was proportional to magma pressure, possibly due to crystallization-induced vesiculation in the feeding magma body. We further suggest that the effusion rate decline could correspond to a gradual slowing of magma intrusion into the source region, progressive solidification of the crystallizing magma reservoir, increasing resistance faced by the magma in getting up the conduit to the surface due to cooling-induced crystallization, greater degassing en route to the surface through a taller and stronger dome, or some combination of these processes. The exogenous lobe production rate similarly dropped rapidly from the first to the second phase and again, but less drastically, from the second to third phase. The sub-parallel trends of total and exogenous growth rates during the later stages of dome growth suggest that the controls on when and how much magma made its way up the conduit also determined the amount of lava that would end up breaking its way to the surface following periods of dome inflation.

In contrast, Fig. 1 shows that endogenous injection did not follow the same overall decreasing trend as exogenous lobe production. Rather, this inflation increased steadily throughout the entire 6-year emplacement of the dome. Fink et al. (1990) suggested that as lava was added episodically to the dome's interior or onto its surface in a piecemeal fashion to create a larger pile, the dome's internal isotherms were affected less by each successive dome growth event. Figure 2 shows the overall development of the dome in profile view, based on photos taken by the USGS from a fixed point 1 km north of the center of the dome.

The steady inward migration of isotherms within the dome would result in an internal boundary layer or crust that had to break to allow exogenous lobes to form. As

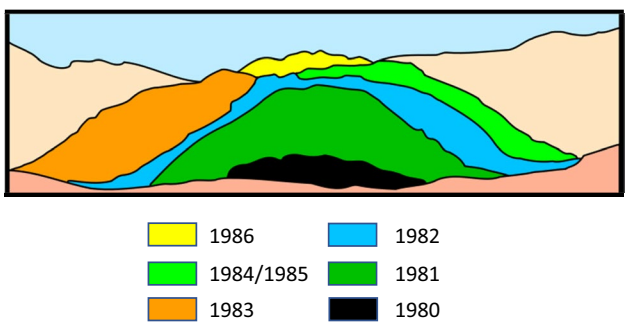

Fig. 2 Schematic drawing of 1980–1986 Mount St. Helens dome growth based on photos taken by USGS from a fixed point 1 km north of the center of the dome. Profiles shown represent the appearance at the end of each time period

pointed out by Denlinger (1990), the tension required for fracturing this zone would be highest at the top of the dome, consistent with the observation that late-stage exogenous lobes tended to appear at the dome's apex. Anderson et al. (2005) and Bull et al. (2013) also pointed out that a unit of lava injected into a small dome will disrupt the surface more than a large dome. This suggests that as the MSH dome grew larger, a greater volume of endogenous growth would be needed to break a viable pathway to the surface to form the exogenous component of the eruption. Fink et al. (1990) concluded that the distinction between exogenous and endogenous growth rates reflected the fact that the former was controlled by processes occurring in the magma body at depth, while the latter was mostly influenced by near-surface cooling of the dome.

Another way to think about the divergence in endogenous and exogenous growth rates, as well as the episodic behavior of the eruption, is to consider the thermal evolution of the mushroom-shaped system comprising the dome and its feeding conduit. For magma to rise into the dome without freezing along the way, the system needs to maintain a temperature above the magma's strain-rate-dependent glass transition temperature. During each eruptive episode, the buoyant magma carries heat that raises the temperature of the wall rocks and the dome that it intrudes. In the hiatus before the next episode, much of this heat can dissipate, increasing the amount of buoyancy needed to initiate the rise of the next batch. These repose periods also tend to lengthen due to the growing height of the dome. The temperature of the conduit will increase in proportion to the frequency of the episodes passing through it and the heat content of their magma pulses.

For the case of the MSH dome, this heating reached a critical level in late 1982, overpowering the cooling that would normally shut off an episode and allowing a much greater volume of lava to erupt continuously over the following year. This episode of continuous effusion indicated that the system retained enough heat to keep the magma in the conduit from solidifying throughout 1983. In contrast, episodic dome growth implied that the generation of buoyant, hot, eruptible magma batches in the near-surface chamber and the cumulative heating of the pathway to the surface were insufficient to prevent periodic cooling of the system, which temporarily shut off the eruption until a new batch of buoyant magma was generated and began rising. The associated delicate feedback between cooling, microlite growth, and viscosity increase has been modeled by Melnik and Sparks (1999) and Barmin et al. (2002). They point out that the nonlinear relations among these processes mean that eruptive style can transition from one state to another quite abruptly with only slight variations in volatile content, complicating forecasting attempts.

Textural evolution of the Mount St. Helens dome

A second aspect of active dome emplacement that was documented and quantified for the first time at Mount St. Helens was the relationship between volatile content and surface textures. All magmas contain gasses that can come out of solution to form bubbles when conditions of temperature and pressure allow. In a typical lava flow, this leads to formation of a vesicular, pumiceous, or scoriaceous surface layer, the thickness of which depends on the lava's viscosity, volatile content, and cooling history. Rapid cooling and/or high viscosities of dome lavas can reduce the diffusivity of volatiles, inhibit the growth of crystals, and in some cases form glassy zones. Crystallization of anhydrous minerals in the hot interior of larger domes can lead to the expulsion of volatiles that can migrate, concentrate, and potentially form zones that can explode into block-and-ash flows if rapidly exposed by gravitational collapse of a flow front, or can violently vent upward to form pits in the upper surface (Manley and Fink 1987; Castro et al. 2002). Fracturing, folding, and jumbling during flow advance can disrupt and obscure the original distribution of surface textures.

Bubbles can change the appearance of the lava in visible, infrared, or radar observations (Ondrusek et al. 1993; Ramsey and Fink 1999). Remote sensing of the vesicular textures preserved on a flow surface can thus provide an indication of otherwise unobserved eruptive conditions. Because both explosive activity and vesiculation are promoted by higher magmatic volatile contents, understanding the relationships between textures and water concentrations can help with hazards assessments. Monitoring scientists need tools that can help them know whether observed shifts in vesicularity during a dome eruption signal that explosive behavior is more or less likely.

The Mount St. Helens dome exhibited two primary textures: *scoriaceous*, with vesicularities of around 25–50% and a rough, lumpy appearance when viewed aerially; and *smooth*, with less than 15% vesicularity and less pronounced decimeter-scale surface topography (Cashman and Taggart 1983; Swanson et al. 1987). Anderson and Fink (1990) used air photos and surface samples to map the distribution of smooth and scoriaceous portions of most of the MSH lobes, in part so that they could identify textural trends that might indicate increasing risk of explosivity. Although more smooth surfaces were seen during later stages of the dome's emplacement, the proportions of the two textures did not vary as systematically with time as did the partitioning between exogenous and endogenous growth shown in Fig. 1.

Comparing textural maps with the evolving topography of the dome showed that smooth textures appeared

when extrusion rates were relatively low, when lava was flowing laterally across relatively shallow surfaces, and when much of the flow surface was dominated by "crease structures" (Anderson and Fink 1990; 1992). Crease structures are fractures that grow downward into a flow surface through a series of incremental cracking events that each rapidly quench a narrow strip of lava, raising its viscosity and slowing or preventing bubble growth, even if volatile contents are relatively high (Anderson and Fink 1992). The paired, stepped, upwardly convex walls of a crease structure result from the accumulation of dozens or more of these parallel, non-vesicular strips. Cooling during crease structure formation takes place mainly along this shallow, few-centimeter-thick zone on the flow surface; if the warmer lava beneath this veneer can vesiculate, it can cause the initially smooth surface to break up and become scoriaceous, hours or days after initial extrusion (Swanson et al. 1987; Swanson and Holcomb 1990; Anderson and Fink 1989; 1990). This pattern of initially smooth texture formation subsequently disrupted by vesiculation, first documented during growth of several of the MSH dome lobes (Cashman and Taggart 1983; Swanson et al. 1987; Anderson and Fink 1990) can be clearly seen in the progression from Fig. 3a to 3b, taken 24 h apart.

Crease structures and associated smooth textures form in places where lava can flow laterally away from an axial crack. They develop early in a dome's history when lava spreads across the crater floor (Fig. 3a); directly over the vent in the early stages of later lobes' development, before they spill down the flow front; or at the final stages, after forward advance of a lobe ends (Fig. 3c and 3d). The observed association between smooth textures and low effusion rates could have at least two explanations: magma rising more slowly through the conduit would tend to lose more gas and emerge with less tendency to vesiculate, or slowly flowing smooth lava would also be less likely to break up into smaller pieces that would more readily vesiculate by increasing the surface area available for degassing. The blocky, mostly smooth surface of the dome in May 1985 (Fig. 3d) is typical of the later stages in the MSH dome growth. Figure 3e is a close view of the September 1984 lobe showing a mix of scoriaceous textures, mostly discolored from degassing, and mostly gray smooth-textured lava.

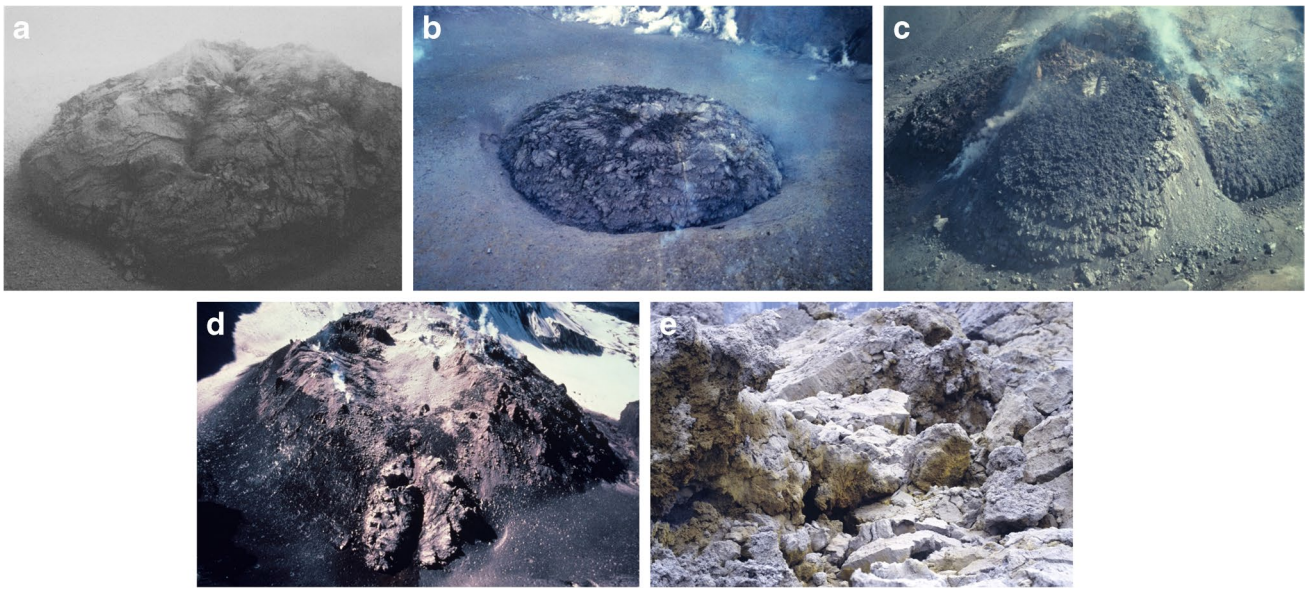

Fig. 3 **a** Looking south into the crater at the lobe-bisecting crease structure in the nearly entirely smooth-textured October 1980 lobe. The lobe is approximately 185 m in diameter (Photo courtesy of the USGS). **b** View looking southwest at the same October 1980 lobe as in **a** but 24 h later. The dome did not grow volumetrically during this time, but the surface changed texture from smooth to scoriaceous (Anderson and Fink 1990), and the dome sagged and widened to approximately 200 m in diameter (Photo courtesy of the USGS). **c** Small smooth-sided crease structure over the vent of the predominantly scoriaceous September 1981 lobe. View is looking to the southwest. The summit crease structure is approximately 25 m across (Photo courtesy of the USGS). **d** View looking NW at the mostly smooth-surfaced May 1985 lobe, showing how the dome became progressively less scoriaceous in the later phases of its growth. **e** Close view of the September 1984 lobe surface showing a mix of scoriaceous textures, mostly discolored from degassing, and mostly gray smooth-textured lava. Width of view is approximately 5 m

Isotopic measurements of volatile contents of the MSH lava dome textures

The distribution of vesicular textures complicates efforts to identify how volatile concentrations vary during a dome eruption. Lava that vesiculates to form scoria would be expected to have initially had higher magmatic water contents. However, demonstrating this relationship by measuring volatiles in vesicular lavas is inherently problematic, because more permeable and porous samples are more likely to be rehydrated by later precipitation (DeGroat-Nelson et al. 2001).

To circumvent this problem, Anderson and Fink (1989; 1990) used hydrogen isotopic measurements of water extracted from fresh MSH dome samples to determine the water's origin. These rocks were collected before they had time to be contaminated by meteoric water. Their δD signatures, measured in water extracted at high temperatures by step-heating, were found to be incompatible with local meteoric values but consistent with magmatic values subjected to open-system, or multi-step open/closed system degassing (Taylor et al. 1983; Taylor 1986). Anderson and Fink (1989) also recognized that as vesiculation caused surface lava to degas to water content levels near 0.1%, a final stage of kinetically controlled volatile loss could occur. This is especially true early in the emplacement of a dome when higher effusion rates combine with low water contents to inhibit exchange between exsolved vapor and the water remaining in the melt (Anderson et al. 1995). Kinetic effects have since been recognized as an important isotope exchange mechanism crucial in high-temperature systems where disequilibrium processes dominate (Watkins and Antonelli 2021).

For several MSH lobes, samples were taken along transects that extended outward from the axis of a crease structure (over the vent) toward the lobe margin; the first-erupted, more distal lava typically displayed the lowest water content values and was assumed to represent the top of the rising magma column that experienced extensive degassing as it slowly broke a path to the dome surface (Anderson and Fink 1990). Water contents in the smooth samples increased from ~ 0.15 to ~ 0.30 wt% from the flow front toward the vent, as shown in Fig. 4 for the May 1986 lobe. Anderson and Fink (1990; 1992) suggested the increase in water content of the smooth samples inward from the flow front resulted from quicker transit through the dome once a path to the surface was created by the lava that eventually ended up near the front of the flow. Directly over the crease axis, where the water contents should have been highest, the smooth lava gave way to a relatively narrow zone of scoria with significantly less water (~ 0.15 wt%). Observation of the flow surface showed that the scoria had vesiculated and broken through the originally

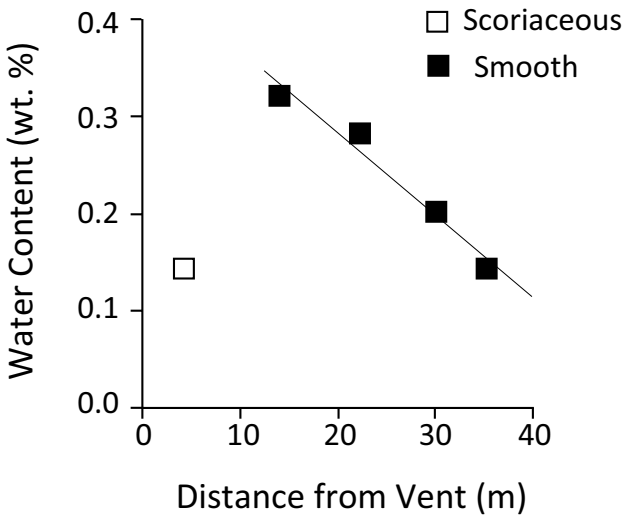

Fig. 4 Water contents of May 1986 lava samples plotted against distance from the vent. From Anderson and Fink 1990

smooth, cooler crease structure surface, consistent with observations that scoriaceous carapaces would form ~ 24 h after extrusion (Anderson and Fink 1990). Anderson and Fink (1990) concluded that this scoria had lost about 0.3 weight percent water when it vesiculated.

Scoriaceous samples collected throughout the lifespan of the dome consistently had water content values in the 0.1–0.2 wt% range, compared to smooth samples ranging from ~ 0.1 to nearly 0.4 wt% (Anderson and Fink 1990; Anderson et al. 1995). These scoriaceous samples therefore represented lava that arrived at the surface with sufficiently high water-contents to cause vesiculation and thorough degassing, whereas the smooth samples had water content values controlled by degassing in the vent and dome interior, but insufficient to cause vesiculation during surface flow (Anderson and Fink 1990). Late stage, smooth-surfaced crease structures that formed toward the end of eruptive episodes may have reflected a slowing of magma ascent, allowing for more extensive degassing of magma prior to its arrival at the surface (Anderson and Fink 1990).

Similar relationships were seen for several of the eruptive phases, implying that volatile contents, and the possibility of associated explosivity, increased during lobe emplacement. Following Swanson and Holcomb (1990), we assume that the first magma to emerge during a given eruptive episode lost volatiles during its rise through the conduit. Because none of these phases ended with explosive activity, we conclude that the residual volatiles generated at depth that resulted in buoyancy were insufficient to fragment the lava when it arrived at the surface. For each of the eruptive episodes, we are assuming that the magma that generated the lobe-forming lava of both textures has the same overall composition, with textural variations reflecting differences

in eruptive conditions and volatile contents, not major or minor element chemistry.

We were able to apply some of the lessons learned from the MSH dome isotope and texture studies to the Santiaguito dome complex in Guatemala, finding similar trends of increasing water content during individual eruptive phases in 45 samples collected over the 70-year duration of the eruption (Anderson et al. 1995). In addition, Bull et al. (2013) noted that after 8 months of activity at Mount Redoubt, where lava domes were subsequently destroyed by explosions, the fourth and final lava dome displayed a carapace with vesicularities over 65%, some of the highest ever recorded for a lava dome. They suggested that the stability of the final lava dome resulted from sufficient fracturing of the conduit to allow for enough degassing en route to the surface to avoid another explosion, illustrating the delicate balance between ascent and degassing rates. They, like Swanson and Holcomb (1990) for Mount St. Helens, suggested that the dome stopped growing when it reached sufficient height for the lithostatic load to offset the buoyant rise of magma.

Surface structures and rheology of the MSH dome

Besides revealing new relationships about eruption mode and texture, the 1980–1986 MSH dome provided novel insights about the meaning of overall dome structure. Over its 6 years of activity, the dome's 18 episodes produced a diverse catalog of morphologies. In some cases, a single lobe spread radially away from a point source, producing a uniform, circular structure with a mostly scoriaceous surface. Some of these relatively low domes had small, discontinuous compressional surface ridges paralleling the flow margins. For example, the September 1981 lobe showed distinct surface folds, or "ogives" that formed as the downslope-flowing front of the lobe decreased in velocity from 1.6 m/h on September 7 to 0.3 m/h from September 8 to 10, and then to 0.1 m/h on September 11, the final day of extrusion. This relationship suggested that folding occurred in a compressional regime created as the main body of the flow continued to move downward while the lava front stagnated (Swanson et al. 1987). This is at odds with a recent suggestion that regularly spaced ridges on silicic extrusions form in an extensional regime (Andrews et al. 2021).

In other cases, like December 1980, a single eruptive phase generated two distinct elliptical-shaped lobes that each moved in a different direction. As already described, several lobes exhibited crease structures, which could form either at the outset (October 1980, September 1981), at the end (June 1981, September 1981), or throughout emplacement (September 1984, May 1985, May 1986), depending on how steep the underlying topography was (Anderson and Fink 1992). Other lobes (September 1981, April 1983) had a variety of fracture types oriented parallel or perpendicular to the flow direction, giving the upper surface a platy appearance. In a few cases, spines were observed over the vent at an early (i.e., April 1981) or late (i.e., February 1983) stage of an episode. Lobe growth was also accompanied by varying proportions of endogenous inflation (Fink et al. 1990).

At the time the MSH dome was active, this set of observations was difficult to interpret, because there was no comprehensive model that could account for all the different morphologies. Over the following decade, Griffiths and Fink conducted an extensive series of laboratory simulations using non-Newtonian mixtures of kaolin powder and polyethylene glycol wax that replicated the rheology and all the above morphological characteristics of domes (Griffiths and Fink 1997; Fink and Griffiths 1998). By varying the experimental conditions, these studies showed that these morphologic types could be organized into a sequence, depending on the ratio of eruption rate to cooling rate, which corresponds to the growth rate of a solidifying crust. The most slowly erupting (or most rapidly cooled) analog extrusions, with the thickest and strongest crusts, produce spines. Slightly faster extrusion rates (or slower cooling rates) yield lobes dominated by fracture processes, including crease structures and large flat-sided plates of smooth lava. Still faster-erupted extrusions have "lobate" morphology with compressional folds along the margins. The highest flow rates result in relatively circular domes of relatively low relief capable of growing by endogenous inflation. The occurrence of specific structures like spines or folds reflects the conditions at the time they formed, not the average conditions over the active duration of a lobe.

Fink and Griffiths (1998) placed these silicic dome types into four categories of increasing eruption rates and/or decreasing cooling rate: "spiny," "platy," "lobate," and "axisymmetric." A given set of eruptive conditions that generates a particular morphology would plot on a field defined by the ratio (Ψ_B) of solidification (t_s) to advection (t_A) timescales,

$$\Psi_B = t_S/t_A = (g\Delta\rho/\sigma_0)^3 Q t_S$$

where g is the gravitational acceleration, $\Delta\rho$ is the density difference between the flow and its ambient environment, σ_0 is the bulk shear strength of the lava, and Q is the effusion rate. Large values of Ψ_B imply that solidification is slow, or eruption rate is high. Thus, the above sequence from spiny to axisymmetric domes corresponds to increasing Ψ_B values.

To see how well the lab-based classification scheme applies to natural domes, Fink and Griffiths (1998) used field observations from eight dome eruptions: Mount St. Helens (USA), Soufrière (St. Vincent), Soufrière Hills Volcano (Montserrat), Pinatubo (Philippines), Merapi

(Indonesia), Unzen (Japan), Santiaguito (Guatemala), and Redoubt (USA). Their conclusion was that if two of three key variables are known (eruption rate, composition/rheology, morphology), the third can be constrained. Thus, if morphology and eruption rate are measured for an active dome, then the effective rheological properties that control emplacement can be determined. If morphologic and compositional information (the latter helping to constrain rheology) are available (e.g., for a prehistoric dome eruption), then paleo-eruption rates can be estimated. The abundance of data collected at Mount St. Helens between 1980 and 1986 allowed this approach to be carefully evaluated and added to the collection of earlier, simpler models available to volcanologists. This builds upon earlier analog studies that sought to explain the structures found on more mafic flows (Fink and Griffiths 1990; Griffiths and Fink 1992), including interpretations of emplacement conditions for submarine (Gregg and Fink 1995) and extraterrestrial lava flows (Griffiths and Fink 1992).

Hazard implications

Deadly pyroclastic density currents may form from the collapse of oversteepened lava dome flow fronts, such as those observed at Mount Unzen in 1991 (Nakada et al. 1995). However, others are propelled by gravitational failure combined with endogenic explosions caused by sudden expansion of volatiles as a flow-front collapses or if pressure is otherwise abruptly released. This latter process was proposed for a 1973 pyroclastic flow that emanated from the foot of a dacite flow at Santiaguito, several kilometers from the vent (Rose et al. 1976). Harnett et al. (2019) compiled a worldwide database of dome collapse events and found that the largest events (those that resulted in the destruction of more than half the lava dome) were those where gravitational loading and gas overpressure followed a period of endogenous growth. Each of the three sets of dome characteristics described above (eruptive style, textures, structures) has implications for this latter style of explosive hazards.

During endogenous dome growth, which tends to happen close to an eruptive vent, lava does not get exposed to the atmosphere, reducing the chances that its volatiles can be lost violently. On the other hand, domes growing by inflation, particularly in a flat-floored crater like at Mount St. Helens, are less likely to collapse, making them inherently safer than those with exogenous lobes flowing downslope.

Scoriaceous lava textures are associated with higher water contents, so their appearance suggests greater explosive risk. At Mount St. Helens, scoria was seen more commonly earlier in the eruption. Scoriaceous textures were also found in lava that displayed a blocky carapace (Anderson et al. 1998), which offered more opportunities for volatiles to escape.

Dome morphologies and structures associated with higher eruption rates, lower cooling rates, and lower viscosities tend to have axisymmetric geometries, surface folds, and smaller surface blocks, all of which indicate higher volatile contents and more chance for explosive behavior. In contrast, domes with spines and crease structures reflect lower volatile contents and conditions less conducive to explosive behavior.

Conclusions

The 1980–1986 eruption at Mount St. Helens provided an unprecedented opportunity to develop and evaluate new models for lava dome growth. The large number of scientists able to access the crater relatively safely over an extended period, along with the availability of substantial instrumentation campaigns led to several new insights about effusive eruptions, which would later be applied to other dome-forming eruptions, including Unzen (Japan), Soufrière Hills (Montserrat), Puyehue-Cordón Caulle (Chile), and the 2004–2008 revival of Mount St. Helens.

We have highlighted three under-appreciated relationships delineated from observations of the Mount St. Helens dome, which might be usefully applied to future eruptions. The first is the surprising way that growth was partitioned between endogenous and exogenous styles, determined from detailed topographic maps. Endogenous additions to the dome volume followed a linear trend over 6 years, despite the formation of more than a dozen different lobes during this period. In contrast, exogenous growth paralleled the tripartite trend in overall volume increases. We interpret this difference as being due to separate controls on the two modes: endogenous growth is limited by the regular inward migration of isotherms in the complex dome, while exogenous growth reflects eruptive conditions in the source magma body and conduit, a conclusion also suggested for a similar growth pattern observed during the emplacement of the Mount Unzen dome (Kaneko et al. 2002). It would be instructive to try to replicate these measurements during future dome-forming eruptions, to determine if the pattern observed at Mount St. Helens and Mount Unzen is unique.

Mapping the variations in vesicular lava textures holds the promise of providing an early warning that a dome might experience endogenic explosive activity. Textural variations in the MSH dome were limited to two main types, smooth and scoriaceous. While the more vesicular, scoriaceous texture would be assumed to require higher volatile contents, demonstrating this relationship

is compromised by the tendency for vesicular samples to become rehydrated by meteoric water. To overcome this complication, we carried out hydrogen isotopic measurements of water extracted from smooth and scoriaceous samples through stepwise heating. The δ D values showed that all measured water was magmatic in origin. Sample profiles taken from the distal flow front to the near-vent areas of several lobes showed that water contents in the smooth samples tended to increase toward the vent until they reached a critical value at which vesiculation and scoria-formation occurred. Although the overall trend was for smooth textures to become more common as the dome grew larger, suggesting a long-term drying out of the source magma body, individual eruptive phases tended to show late-stage increases in volatiles, with associated increased risk of explosivity. Comparison with measurements of hydrogen isotopes and water content for samples from the Santiaguito dome complex in Guatemala showed a similar pattern.

The overall morphology of a dome lobe can provide a third source of insight about eruptive processes. As quantified in laboratory simulations and confirmed at Mount St. Helens, the variety of surface structures (fractures, spines, folds) and textures (smooth or scoriaceous) found on domes can be placed into a continuum based on the ratio of how quickly a flow cools relative to how quickly it advances. If two of three key variables (eruption rate, composition/rheology, morphology) are known, the third can be estimated. Since certain structures and textures indicate that gasses are more or less likely to become concentrated in a flow, their appearance can hint at increased hazards of endogenic explosions.

In retrospect, the overarching value of the 1980–1986 Mount St. Helens dome eruption came from the potential it offered of combining many different types of observations to develop new models. Future dome eruptions will allow these and other models to be tested and refined, especially if they are observed with new, more advanced techniques including drones, higher-resolution satellite and aircraft-based imaging, or cheaper environmental sensors. This progress in instrumentation is complemented by advances in communications; the ability of scientists from around the world to simultaneously observe active domes in near-real time should accelerate the generation of important new insights.

Acknowledgements Our original work at Mount St. Helens in the 1980s could not have been accomplished without the generous assistance of Donald Swanson, Robin Holcomb, Dan Dzurisin, Fred Swanson, and their colleagues at the US Geological Survey and US Forest Service. Two helpful reviews by Jackie Kendrick and an anonymous referee significantly improved the manuscript.

Funding Research was funded by grants from the National Science Foundation and NASA.

References

Anderson SW, Fink JH (1989) Hydrogen-isotope evidence for extrusion mechanisms of the Mount St. Helens dome. Nature 341:521–523

Anderson SW, Fink JH (1990) The development and distribution of lava textures at the Mount St. Helens dome. In: Fink J (ed) The mechanics of lava flow and dome growth, IAVCEI proceedings in volcanology, vol 2. Springer, Heidelberg, pp 25–46

Anderson SW, Fink JH (1992) Crease structures: indicators of emplacement rates and surface stress regimes of lava flows. Geol Soc Am Bull 104(5):615–625

Anderson SW, Fink JH, Rose WI (1995) Mount St. Helens and Santiaguito lava domes: the effect of short-term eruption rate on surface texture and degassing processes. J Volcanol Geotherm Res 69:105–116

Anderson SW, Stofan ER, Plaut JJ, Crown DA (1998) Block size distributions on silicic lava flow surfaces: implications for emplacement conditions. Geol Soc Am Bull 110:1258–1267

Anderson SW, McColley S, Fink JH, Hudson R (2005) The development of fluid instabilities and preferred pathways in lava flow interiors: insights from analog experiments and fractal analysis. In: Manga M, Ventura G (eds) Kinematics and dynamics of lava flows, vol 396. Geological Society of America Special Paper, pp 147–161. https://doi.org/10.1130/2005.2396(10)

Andrews GDM, Kenderes SM, Whittington AG, Isom SL, Brown SR, Pettus HD, Cole BG, Gokey KJ (2021) The fold illusion: the origins and implications of ogives on silicic lavas. Earth Planet Sci Lett 553:116643

Barmin A, Melnik O, Sparks RSJ (2002) Periodic behavior in lava dome eruptions. Earth Planet Sci Lett 199(1–2):173–184

Blake S (1990) Viscoplastic models of lava domes. In: Fink J (ed) The mechanics of lava flow and dome growth, IAVCEI proceedings in volcanology, vol 2. Springer, Heidelberg, pp 88–126

Boudon G, Balcone-Boissard H (2021) Volcanological evolution of Montagne Pelée (Martinique): a textbook case of alternating Plinian and dome-forming eruptions. Earth Sci Rev 221:103754

Bull KF, Buurman H (2013) An overview of the 2009 eruption of redoubt volcano, Alaska. J Volcanol Geotherm Res 259:2–15

Bull KF, Anderson SW, Diefenbach A, Wessel RL, Henton S (2013) Emplacement of the final lava dome of the 2009 eruption of redoubt volcano, Alaska. J Volcanol Geotherm Res. https://doi.org/10.1016/j.jvolgeores.2012.06.014

Burzynski AM, Anderson SW, Morrison K, Patrick M, Orr T, Thelen W (2018) Lava lake thermal pattern classification using self-organizing maps and relationships to eruption processes at Kīlauea volcano, Hawaii. In: Poland M, Garcia M, Camp V, Grunder A (eds) Field volcanology: a tribute to the distinguished career of Don Swanson: Geological Society of America special paper, vol 538, pp 307–324. https://doi.org/10.1130/2018.2538(14)

Calder ES, Lavallée Y, Kendrick JE, Bernstein M (2015) Lava dome eruptions. In: The encyclopedia of volcanoes. Academic Press, pp 343–362

Cashman KV (1992) Groundmass crystallization of Mount St. Helens dacite, 1980–1986: a tool for interpreting shallow magmatic processes. Contrib Mineral Petrol 109(4):431–449

Cashman KV, Taggart JE (1983) Petrologic monitoring of 1981 and 1982 eruptive products from mount St. Helens. Science 221(4618):1385–1387

Castro JM, Cashman KV, Joslin N, Olmsted B (2002) Structural origin of large gas cavities in the big obsidian flow, Newberry volcano. J Volcanol Geotherm Res 114(3–4):313–330

Castro JM, Schipper CI, Mueller SP, Militzer AS, Amigo A, Parejas CS, Jacob D (2013) Storage and eruption of near-liquidus rhyolite magma at Cordón Caulle, Chile. Bull Volcanol 75(4):1–17

Chadwick WW Jr, Swanson DA (1989) Thrust faults and related structures in the crater floor of Mount St. Helens volcano, Washington. Geol Soc Am Bull 101(12):1507–1519

Colombier M, Bernard B, Wright H, Le Pennec JL, Cáceres F, Cimarelli C, Heap MJ, Samaniego P, Vassuer J, Dingwell DB (2022) Conduit processes in crystal-rich dacitic magma and implications for eruptive cycles at Guagua Pichincha volcano, Ecuador. Bull Volcanol 84(12):105

Coombs ML, Bull KF, Vallance JW, Schneider DJ, Thoms EE, Wessels RL, McGimsey RG (2006) Timing, distribution, and volume of proximal products of the 2006 eruption of Augustine volcano. In: USGS professional paper 1769, the 2006 eruption of Augustine volcano, Alaska, pp 145–186

DeGroat-Nelson PJ, Cameron BI, Fink JH, Holloway JR (2001) Hydrogen isotope analysis of rehydrated silicic lavas: implications for eruption mechanisms. Earth Planet Sci Lett 185(3–4):331–341

Denlinger, RP (1990) A model for dome eruptions at Mount St. Helens, Washington based on subcritical crack growth, in Fink, J. (ed) The mechanics of lava flow and dome growth, IAVCEI proceedings in volcanology, vol 2. Springer, Heidelberg, pp 70–87

Eichelberger JC, Carrigan CR, Westrich HR, Price RH (1986) Nonexplosive silicic volcanism. Nature 323(6089):598–602

Farquharson JI, James MR, Tuffen H (2015) Examining rhyolite lava flow dynamics through photo-based 3D reconstructions of the 2011–2012 lava flow field at Cordón-Caulle, Chile. J Volcanol Geotherm Res 304:336–348

Fink JH (ed) (1990) The mechanics of lava flow and dome growth, IAVCEI proceedings in volcanology 2. Springer, Heidelberg

Fink JH, Griffiths RW (1990) Radial spreading of viscous-gravity currents with solidifying crust. J Fluid Mech 221:485–509

Fink JH, Griffiths RW (1998) Morphology, eruption rates, and rheology of lava domes: insights from laboratory models. J Geophys Res Solid Earth 103(B1):527–545

Fink JH, Pollard DD (1983) Structural evidence for dikes beneath silicic domes, medicine Lake Highland volcano, California. Geology 11(8):458–461

Fink JH, Malin MC, Anderson SW (1990) Intrusive and extrusive growth of the mount St Helens lava dome. Nature 348(6300):435–437

Fink JH, Anderson SW, Manley CR (1992) Textural constraints on effusive silicic volcanism: beyond the permeable foam model. J Geophys Res Solid Earth 97(B6):9073–9083

Gregg TKP, Fink JH (1995) Quantification of submarine lava-flow morphology through analog experiments. Geology 23(1):73–76

Griffiths RW, Fink JH (1992) The morphology of lava flows in planetary environments: predictions from analog experiments. J Geophys Res 97(B13):19739–19748

Griffiths RW, Fink JH (1997) Solidifying Bingham extrusions: a model for the growth of silicic lava domes. J Fluid Mech 347:13–36

Harnett CE, Thomas ME, Calder ES, Ebmeier SK, Telford A, Murphy W, Neuberg J (2019) Presentation and analysis of a worldwide database for lava dome collapse events: the global archive of dome instabilities (GLADIS). Bull Volcanol 81:1–17

Harris AJ, Rose WI, Flynn LP (2003) Temporal trends in lava dome extrusion at Santiaguito 1922–2000. Bull Volcanol 65(2):77–89

Hoblitt RP, Harmon RS (1993) Bimodal density distribution of cryptodome dacite from the 1980 eruption of Mount St. Helens, Washington. Bull Volcanol 55:421–437

Huppert HE, Shepherd JB, Sigurdsson H, Sparks RSJ (1982) On lava dome growth, with application to the 1979 lava extrusion of the Soufriere of St. Vincent. J Volcanol Geotherm Res 14(3–4):199–222

Ikegami F, McPhie J, Carey R, Mudana R, Soule A, Jutzeler M (2018) The eruption of submarine rhyolite lavas and domes in the deep ocean–Havre 2012, Kermadec Arc. Front Earth Sci 6:147

Iverson RM (1990) Lava domes modeled as brittle shells that enclose pressurized magma, with application to Mount St. Helens. In: Fink J (ed) The mechanics of lava flow and dome growth, IAVCEI proceedings in volcanology, vol 2. Springer, Heidelberg, pp 47–69

Kaneko T, Wooster MJ, Nakada S (2002) Exogenous and endogenous growth of the Unzen lava dome examined by satellite infrared image analysis. J Volcanol Geotherm Res 116(1–2):151–160

Koenig E, Fink JH (2002) The volcano listserv and its use in education, vol 2002. AGU Spring Meeting Abstracts, pp V51C–V506C

LeWinter AL, Anderson SW, Finnegan DC, Patrick MR, Orr TR (2021) Crater growth and lava-lake dynamics revealed through multitemporal terrestrial lidar scanning at Kīlauea volcano, Hawai'i. In: Patrick M, Orr T, Swanson DA, Houghton B (eds) USGS professional paper 1867-C, the 2008–2018 Summit Lava Lake at Kīlauea volcano, Hawai'i, vol 26. https://doi.org/10.3133/pp1867C

Luhr JF, Carmichael IS (1980) The Colima volcanic complex, Mexico: I. post-caldera andesites from Volcán Colima. Contrib Mineral Petrol 71:343–372

Lyman AW, Koenig E, Fink JH (2004) Predicting yield strengths and effusion rates of lava domes from morphology and underlying topography. J Volcanol Geotherm Res 129(1–3):125–138

Manley CR, Fink JH (1987) Internal textures of rhyolite flows as revealed by research drilling. Geology 15(6):549–552

Melnik O, Sparks RSJ (1999) Nonlinear dynamics of lava dome extrusion. Nature 402(6757):37–41

Melnik O, Sparks RSJ (2005) Controls on conduit magma flow dynamics during lava dome building eruptions. J Geophys Res Solid Earth 110(B02209)

Nakada S, Miyake Y, Sato H, Oshima O, Fujinawa A (1995) Endogenous growth of dacite dome at Unzen volcano (Japan), 1993–1994. Geology 23(2):157–160

Nakada S, Shimizu H, Ohta K (1999) Overview of the 1990–1995 eruption at Unzen volcano. J Volcanol Geotherm Res 89(1–4):1–22

Ondrusek J, Christensen PR, Fink JH (1993) Mapping the distribution of vesicular textures on silicic lavas using the thermal infrared multispectral scanner. J Geophys Res Solid Earth 98(B9):15903–15908

Pallister JS, Diefenbach AK, Burton WC, Muñoz J, Griswold JP, Lara LE, Lowenstern JB, Valenzuela CE (2013) The Chaitén rhyolite lava dome: eruption sequence, lava dome volumes, rapid effusion rates and source of the rhyolite magma. Andean Geol 40(2):277–294

Pappalardo RT, Greeley R (1995) A review of the origins of subparallel ridges and troughs: generalized morphological predictions from terrestrial models. J Geophys Res Planets 100(E9):18985–19007

Quick LC, Fagents SA, Núñez KA, Wilk KA, Beyer RA, Beddingfield CB, Martin ES, Prockter LM, Hurford TA (2022) Cryolava dome growth resulting from active eruptions on Jupiter's moon Europa. Icarus 387:115185

Rampey ML, Milam KA, McSween HY Jr, Moersch JE, Christensen PR (2007) Identity and emplacement of domical structures in the western Arcadia Planitia, Mars. J Geophys Res Planets 112(E6)

Ramsey MS, Fink JH (1999) Estimating silicic lava vesicularity with thermal remote sensing: a new technique for volcanic mapping and monitoring. Bull Volcanol 61(1):32–39

Ramsey MS, Wessels RL, Anderson SW (2012) Surface textures and dynamics of the 2005 Shiveluch volcano, Kamchatka. Geol Soc Am Bull 124:678–689. https://doi.org/10.1130/B30580.1

Rhodes E, Kennedy BM, Lavallée Y, Hornby A, Edwards M, Chigna G (2018) Textural insights into the evolving lava dome cycles at Santiaguito lava dome, Guatemala. Front Earth Sci 6:30

Romagnoli C, Casalbore D, Bosman A, Braga R, Chiocci FL (2013) Submarine structure of Vulcano volcano (Aeolian Islands) revealed by high-resolution bathymetry and seismo-acoustic data. Mar Geol 338:30–45

Rose WI, Pearson T, Bonis S (1976) Nuée ardente eruption from the foot of a dacite lava flow, Santiaguito volcano, Guatemala. Bulletin Volcanologique 40(1):23–38

Rutherford MJ, Hill PM (1993) Magma ascent rates from amphibole breakdown: an experimental study applied to the 1980-1986 Mount St. Helens eruptions. J Geophys Res Solid Earth 98(B11):19667–19685

Schipper CI, Castro JM, Tuffen H, James MR, How P (2013) Shallow vent architecture during hybrid explosive–effusive activity at Cordón Caulle (Chile, 2011–12): evidence from direct observations and pyroclast textures. J Volcanol Geotherm Res 262:25–37

Sherrod DR, Scott WE, Stauffer PH (eds) (2008) A volcano rekindled: the renewed eruption of Mount St. Helens, 2004–2006. US Geol Surv Prof Pap 1750:225–236

Siebert L, Begét JE, Glicken H (1995) The 1883 and late-prehistoric eruptions of Augustine volcano, Alaska. J Volcanol Geotherm Res 66(1–4):367–395

Sparks RSJ, Young SR (2002) The eruption of Soufrière Hills volcano, Montserrat (1995–1999): overview of scientific results. Geol Soc London Memoirs 21(1):45–69

Stofan ER, Anderson SW, Crown DA, Plaut JJ (2000) Emplacement and composition of steep-sided domes on Venus. J Geophys Res Planets 105:26757–26772

Swanson DA, Holcomb RT (1990) Regularities in growth of the Mount St. Helens dacite dome, 1980–1986, in Fink, J (ed) the mechanics of lava flow and dome growth. IAVCEI Proc Volcanol 2:3–24

Swanson DA, Dzurisin D, Holcomb RT, Iwatsubo EY, Chadwick WW Jr, Casadevall TJ, Ewert JW, Heliker CC (1987) Growth of the lava dome at Mount St. Helens, Washington (USA), 1981–1983 in Fink J (ed) the emplacement of silicic domes and lava flows. Geol Soc Am Spec Pap 212:1–16

Taylor BE (1986) Magmatic volatiles: isotope variation of C, H and S—reviews in mineralogy in stable isotopes in high temperature geological processes. Mineral Soc Am:185–222

Taylor BE, Eichelberger JC, Westrich HR (1983) Hydrogen isotopic evidence of rhyolitic magma degassing during shallow intrusion and eruption. Nature 306(5943):541–545

Tuffen H, James MR, Castro JM, Schipper CI (2013) Exceptional mobility of an advancing rhyolitic obsidian flow at Cordón Caulle volcano in Chile. Nat Commun 4(1):1–7

Underwood SJ, Feeley TC, Clynne MA (2013) Hydrogen isotope investigation of amphibole and glass in dacite magmas erupted in 1980–1986 and 2005 at Mount St. Helens, Washington. J Petrol 54:1047–1070

Wadsworth FB, Llewellin EW, Castro JM, Tuffen H, Schipper CI, Gardner JE, Vasseur J, Foster A, Damby DE, McIntosh IM, Boettcher S, Unwin HE, Heap MJ, Farquharson JI, Dingwell DB, Iacovino K, Paisley R, Jones C, Whattam J (2022) A reappraisal of explosive–effusive silicic eruption dynamics: syn-eruptive assembly of lava from the products of cryptic fragmentation. J Volcanol Geotherm Res 2022:107672

Watkins JM, Antonelli M (2021) Beyond equilibrium: kinetic isotope fractionation in high-temperature environments. Elements: An International Magazine of Mineralogy, Geochemistry, and Petrology 17(6):383–388

Watts RB, Herd RA, Sparks RSJ, Young SR, Druitt TH (2002) Growth patterns and emplacement of the andesitic lava dome at Soufriere Hills volcano, Montserrat. Mem Geol Soc Lond 21:115–152

Widiyantoro S, Ramdhan M, Métaxian JP, Cummins PR, Martel C, Erdmann S, Nugraha AD, Budi-Santoso A, Laurin A, Fahmi AA (2018) Seismic imaging and petrology explain highly explosive eruptions of Merapi volcano, Indonesia. Sci Rep 8(1):1–7

Wilson L, Head JW (2003) Lunar Gruithuisen and Mairan domes: rheology and mode of emplacement. J Geophys Res Planets 108(E2)